LETTER

doi:10.1038/nature11937

Evidence for sympathetic vibrational cooling of translationally cold molecules

Wade G. Rellergert[1], Scott T. Sullivan[1], Steven J. Schowalter[1], Svetlana Kotochigova[2], Kuang Chen[1] & Eric R. Hudson[1]

Compared with atoms, molecules have a rich internal structure that offers many opportunities for technological and scientific advancement. The study of this structure could yield critical insights into quantum chemistry[1–3], new methods for manipulating quantum information[4,5], and improved tests of discrete symmetry violation[6,7] and fundamental constant variation[8–10]. Harnessing this potential typically requires the preparation of cold molecules in their quantum rovibrational ground state. However, the molecular internal structure severely complicates efforts to produce such samples. Removal of energy stored in long-lived vibrational levels is particularly problematic because optical transitions between vibrational levels are not governed by strict selection rules, which makes laser cooling difficult. Additionally, traditional collisional, or sympathetic, cooling methods are inefficient at quenching molecular vibrational motion[11]. Here we experimentally demonstrate that the vibrational motion of trapped $BaCl^+$ molecules is quenched by collisions with ultracold calcium atoms at a rate comparable to the classical scattering, or Langevin, rate. This is over four orders of magnitude more efficient than traditional sympathetic cooling schemes[11]. The high cooling rate, a consequence of a strong interaction potential (due to the high polarizability of calcium), along with the low collision energies involved[12], leads to molecular samples with a vibrational ground-state occupancy of at least 90 per cent. Our demonstration uses a novel thermometry technique that relies on relative photodissociation yields. Although the decrease in vibrational temperature is modest, with straightforward improvements it should be possible to produce molecular samples with a vibrational ground-state occupancy greater than 99 per cent in less than 100 milliseconds. Because sympathetic cooling of molecular rotational motion is much more efficient than vibrational cooling in traditional systems, we expect that the method also allows efficient cooling of the rotational motion of the molecules. Moreover, the technique should work for many different combinations of ultracold atoms and molecules.

Precision control over the quantum states of atoms has allowed tremendous advances in both applied and fundamental physics, ranging from ultraprecise clocks[13] and gravity gradiometers[14], to stringent tests on discrete symmetry violations[15] and the production of exotic phases of matter such as degenerate Bose and Fermi gases[16]. Extension of these studies to the next simplest such physical system, that is, a diatomic molecule, promises even further progress. Typically, the starting point for these studies is the production of an ultracold sample, which in the case of atoms is usually attained by laser cooling. Applying this technique to molecules, however, is technically challenging, owing mainly to the molecular vibrational degree of freedom, which has no associated angular momentum. Thus, unlike transitions between different rotational and electronic levels, transitions between vibrational levels of a molecule are not governed by strict selection rules. As a result, in general, a molecule simply cannot scatter the necessary number of photons needed to enter the ultracold regime before spontaneously decaying to long-lived vibrational levels that are out of resonance with the cooling lasers. Although it does seem that a subset of molecules are potentially amenable to laser cooling, as has been recently demonstrated for SrF (ref. 17) and YO (ref. 18), a more general cooling technique is highly desirable. One promising, general method is to use a sample of laser-cooled ultracold atoms to collisionally, that is, sympathetically, cool a co-trapped sample of molecules to ultralow temperatures. Particularly attractive for this technique are charged molecules, which, in contrast to neutral molecules, can be trapped over a broad temperature range for extended periods of time in radio-frequency ion traps, allowing ample time for sympathetic cooling to occur.

So far, sympathetic cooling of charged molecules has been demonstrated with both laser-cooled atomic ions and cryogenic buffer gases[11]. Unfortunately, neither of these methods can produce molecules that are simultaneously ultracold in both their internal and external degrees of freedom. On the one hand, sympathetic cooling with co-trapped, laser-cooled atomic ions quickly cools molecular ions to very low translational temperatures, but, owing to the long-range nature of the Coulomb interaction, the method yields little internal-state relaxation of the molecules at low collision energies[19]. To overcome this limitation, techniques of optical pumping[20,21] and state-selective photoionization of neutral molecules[22] have been used in tandem with atomic ion sympathetic cooling to produce translationally cold molecular ions in the lowest few rotational states. Despite their impressive results, these techniques lack generality because they are restricted to certain classes of molecule and require molecule-specific lasers. On the other hand, sympathetic cooling with helium buffer gas has been demonstrated to yield cooling of both the translational and internal states of molecules owing to the short-range nature of the ion-neutral collision; however, the method can only be used at temperatures above $\sim$300 mK, the point at which the vapour pressure of ^{3}He becomes negligibly small. Additionally, it is relatively inefficient as a result of the low polarizability of the helium atoms.

An alternative to these methods is sympathetic cooling with ultracold, laser-cooled atoms, which both allows access to submillikelvin translational temperatures and is predicted to be very efficient at cooling the internal degrees of freedom because their polarizabilities are more than 100 times greater than that of helium atoms. Although this scheme uses proven technologies that have existed for decades, it has not previously been implemented, possibly owing to the misconception that molecular ions cannot undergo primarily elastic collisions with neutral atoms that are amenable to laser cooling, but instead undergo charge-exchange chemical reactions leading to energetic, neutral molecules. Previously, we have shown that, on the contrary, many combinations of molecular ions and neutral laser-cooled atoms (including the combination of species used here) can coexist without undergoing a chemical reaction when colliding[23]. Here we present evidence of internal-state cooling of trapped molecular ions due to sympathetic cooling collisions with ultracold atoms co-located in a magneto-optical trap (MOT). Although the demonstrated degree of cooling is modest, the method is found to be extremely efficient, with a vibrational quenching rate constant on the order of the classical, or Langevin, atom–ion scattering rate constant. Thus, straightforward

[1]Department of Physics and Astronomy, University of California, Los Angeles, California 90095, USA. [2]Department of Physics, Temple University, Philadelphia, Pennsylvania 19122, USA.

improvements in the apparatus should allow production of molecular samples in the vibrational ground state in less than 100 ms. In what follows, we detail a novel technique that we have developed to measure relative populations of molecular vibrational levels, briefly describe the apparatus and experimental approach used to sympathetically cool $BaCl^+$ molecules, and present data detailing the measured vibrational sympathetic cooling rate.

To quantify the degree of sympathetic cooling of the molecular internal levels, it is necessary to measure the population distribution of rotational and vibrational levels. Typically, this measurement is accomplished with spectroscopic techniques, such as predissociation or multiphoton ionization/dissociation spectroscopy; however, as for most molecular ions, the detailed spectroscopic information necessary for these techniques is not yet known for $BaCl^+$. To overcome this challenge, we develop a new route to demonstrate vibrational spectroscopic thermometry experimentally, which uses broadband molecular photodissociation and as such does not require detailed molecular structure data. This novel and general method is applicable to any molecule that can be directly photodissociated and allows an accurate measurement of the molecular vibrational temperature, as long as the internal-state population can be probed on a timescale shorter than or comparable to the vibrational relaxation time. The method exploits the fact that, although the photodissociation cross-section is broad, the individual vibrational levels have unique frequency responses for photodissociation, which are given by[24]

$$\sigma_{vJ}(v) = 4\pi^2 \alpha a_0^2 \frac{hv}{E_h} \frac{1}{2J+1} \sum_{J',M,M'} \frac{|\langle A,\varepsilon J'M'|d_z|X,vJM\rangle|^2}{\left(ea_0/\sqrt{E_h}\right)^2}$$

where E_h is the Hartree energy, e is the charge of the electron, a_0 is the Bohr radius, α is the fine-structure constant, h is Planck's constant, hv is the photon energy, ε is the energy of the continuum wavefunction and v is the vibrational quantum number of the X state. The rovibrational wavefunctions of the ground state, $^1\Sigma^+$, and first electronic excited state, $^1\Pi$ (Fig. 1a), are respectively denoted $|X\rangle$ and $|A\rangle$, with rotational quantum numbers J and J', which have space-fixed z-axis projections of M and M'. The quantity $\langle A|d_z|X\rangle / \left(ea_0/\sqrt{E_h}\right)$ is dimensionless and contains both the radial and angular parts of the dipole moment, d. Because the continuum wavefunctions associated with solutions of the $A^1\Pi$ molecular potential are highly oscillatory, the expectation value of the dipole moment operator can be accurately approximated by considering only the nature of $|A\rangle$ near the classical turning point, R_C. Thus, if the repulsive potential is approximated as being linearly dependent on R, with slope dV_A/dR, near $R = R_C$, these wavefunctions are well described by Airy functions and the vibrational photodissociation cross-section is given by

$$\sigma_{vJ}(v) = \frac{4\pi^2\alpha}{e^2} \frac{hv}{2J+1} \left(d(R_C) \frac{\phi_v(R_C)}{\sqrt{dV_A/dR|_{R=R_C}}} \right)^2 \qquad (1)$$

where ϕ_v are the real-valued vibrational wavefunctions. Because R_C is linearly related to the photon energy, the shape of the photodissociation cross-section directly reflects the squared probability amplitude of the molecular vibrational wavefunction.

Implementing the photodissociation thermometry technique to be discussed requires knowledge of a photodissociation transition from which an accurate determination of the ϕ_v can be obtained. Recently, we identified such a photodissociation transition in $BaCl^+$ (ref. 24). However, to implement the thermometry technique, it was necessary to measure the shape of the photodissociation cross-section to higher precision. To this end, we have developed a novel, compact time-of-flight apparatus[25], which enabled us to measure the photodissociation spectrum of $BaCl^+$ about 1,000 times more precisely than in ref. 24. From this data (Fig. 1c), slight adjustments to the molecular potentials determined in ref. 24 have been made, and the contributions

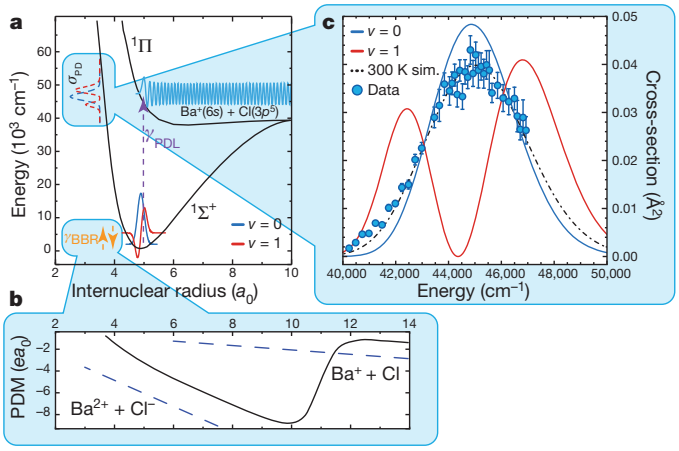

Figure 1 | Photodissociation thermometry of $BaCl^+$. **a**, Potential energy curves for the $X^1\Sigma^+$ and $A^1\Pi$ electronic states and a schematic diagram indicating the photodissociation thermometry method described in the text. The different shapes of the $v = 0$ and $v = 1$ wavefunctions give rise to the different frequency responses of the two levels to the photodissociation laser. γ_{BBR}, redistribution rate due to black-body radiation; γ_{PDL}, transition rate due to the photodissociation laser given the cross-section σ_{PD}. **b**, The permanent dipole moment (PDM) of $BaCl^+$ calculated as described in Methods. **c**, Improved data (errors, s.e.) obtained for the cross-section of the $A^1\Pi \leftarrow X^1\Sigma^+$ photodissociation transition in $BaCl^+$ using a separate ion trap and time-of-flight system. The dash–dot line is the thermally averaged cross-section at 300 K. Also shown are the improved calculations of the individual vibrational-level contributions of the $v = 0$ and $v = 1$ levels. Although our model (Methods) incorporates the lowest four vibrational levels, here we show only the $v = 0$ and $v = 1$ levels, for clarity.

of the individual vibrational states to the total photodissociation cross-section can be identified, the lowest two of which (that is, $v = 0$ and $v = 1$) are shown as solid lines in Fig. 1c.

With the individual vibrational-level cross-sections in hand, the crux of the thermometry technique can be understood as follows. Once equilibration has been established with the vacuum apparatus, which operates at 300 K, ~79% of the molecules are in the $v = 0$ level, ~15% are in the $v = 1$ level and the remaining population is essentially all in the $v = 2$ and $v = 3$ levels. Although the model introduced later incorporates all of these levels, for illustrative purposes it is sufficient to consider only the $v = 0$ and $v = 1$ levels. Because the wavefunction of the $v = 1$ level has a zero crossing (Fig. 1a) the photodissociation cross-section contains a node (Fig. 1b), which occurs at $\lambda = 225$ nm ($v/c = 44{,}400$ cm^{-1}). A laser tuned to this wavelength will photodissociate molecules in the $v = 0$ level, but will not affect molecules in the $v = 1$ level. Furthermore, as can be inferred by thermally averaging equation (1), at the temperatures relevant to this work the rotational distribution does not change the resulting cross-sections. As a result, if collisions with the ultracold Ca atoms quench the vibrational motion of the molecules, this quenching will be signalled by an enhanced photodissociation rate at this wavelength. Conversely, by tuning the photodissociation laser (PDL) closer to one of the maxima of the $v = 1$ cross-section, MOT-induced quenching will instead be signalled by suppression of the observed photodissociation rate as molecules are being cooled to the $v = 0$ level, lowering the total cross-section. As a result, we can infer the change in vibrational temperature from the change in photodissociation rate at different photodissociation wavelengths.

The hybrid atom–ion apparatus, which we call the MOTion trap, used to measure these effects is similar to the one used in refs 26, 27 (a detailed schematic diagram can be found in Supplementary Information). Typical data obtained to demonstrate vibrational cooling is plotted in Fig. 2a. To begin, $BaCl^+$ molecules created by laser ablation are trapped in a linear quadrupole ion trap (Fig. 2a, i), which is co-located with a MOT that can be loaded with ultracold Ca atoms. Notably, without any cooling, the initial internal and translational

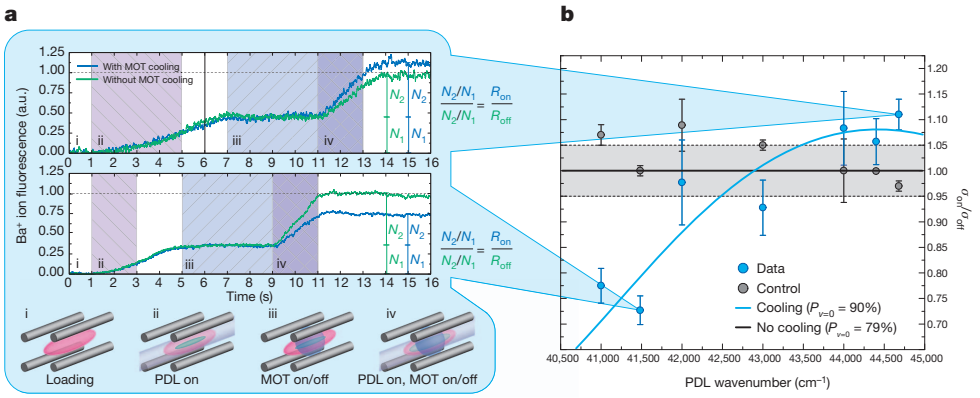

Figure 2 | Measurement of MOT-induced vibrational quenching of $BaCl^+$ ions. **a**, Example traces of the Ba^+ ion fluorescence measured during the experimental sequence. Initially the trap is loaded with a pure $BaCl^+$ sample (pink) (i). The PDL is then turned on to create a mixed sample of $BaCl^+$ and Ba^+ ions (green) (ii). Once the Ba^+ ions have been laser-cooled, the MOT (blue) is optionally turned on and the $BaCl^+$ ions are collisionally cooled by the ultracold Ca atoms (iii). Following that, the $BaCl^+$ ions are probed with the PDL to determine the amount of vibrational relaxation due to the MOT (iv). The ratio of the numbers of Ba^+ ions created in each instance of photodissociation with the MOT respectively on or off is then calculated. The top and bottom panels are data for PDL wavenumbers of 41,500 and 44,675 cm^{-1}, respectively. a.u., arbitrary units. **b**, The average of all data points (errors, s.e.) obtained, as described in Methods, is plotted for various photodissociation wavenumbers. The blue points are cooling data and the grey points are a control analysis that should be consistent with unity (Methods). The curves are the expected result from a rate equation model of the experimental sequence described in Methods. The agreement with the data shows that the $BaCl^+$ sample has been cooled to a ground-state vibrational population of ~90% in the average case.

temperatures of the $BaCl^+$ molecules are determined by different mechanisms and are established in the first few seconds after the trap is loaded. Internally, the $BaCl^+$ molecules thermalize to 300 K owing to black-body radiation emitted by the room-temperature vacuum apparatus, while translationally the temperature is set by the ion dynamics in the trap. To attain measurements with the high signal-to-noise ratio necessary to demonstrate vibrational cooling, the system requires the use of an ion cloud composed of $\sim 10^3$ $BaCl^+$ molecules. At these numbers, the initial translational temperature of the $BaCl^+$ molecules is primarily set to ~1,000 K by collisional heating through micromotion interruption, which results when collisions between ions disrupt the stable ion trajectories in the trap allowing the radio-frequency confining potential to do net work on the ions[28]. Therefore, for this experiment, we use additional translational cooling of the $BaCl^+$ molecules by sympathetic cooling with co-trapped, laser-cooled Ba^+ ions. These Ba^+ ions are loaded into the trap with 100% efficiency by photodissociating a fraction of the $BaCl^+$ molecules using a pulsed dye laser as discussed in ref. 24 (Fig. 2a, ii), and, once laser-cooled, sympathetically cool the $BaCl^+$ molecules to millikelvin translational temperatures[19].

These atomic ions also provide an important diagnostic, because their fluorescence is used both as a means of determining overlap of the MOTion trap[26] as well as the initial, proportional number of $BaCl^+$ molecules.

Once the $BaCl^+$ molecules are translationally cold, as indicated by the steady-state value of the Ba^+ ion fluorescence and camera images of the ion cloud, the MOT is turned on (Fig. 2a, iii) and short-range collisions with the highly polarizable, neutral Ca atoms result in internal-state cooling. To measure the effect of the cooling, the PDL is then turned on once again (Fig. 2a, iv) and the increase in fluorescence yields the number of Ba^+ ions produced, thus allowing an inference of the ground-state vibrational population of the $BaCl^+$ molecules.

Several sources of systematic error can be eliminated (for example the variable number of $BaCl^+$ molecules produced in the loading process and possible inaccuracies in the absolute cross-section value, the PDL intensity or both) by taking the ratio of the final number of Ba^+ ions produced to the initial number, $R_{on} = N_2/N_1$ (Methods and Fig. 2a). We then repeat this measurement sequence without turning on the Ca MOT and determine the same ratio, which we denote R_{off}. It is straightforward to show that in the linear regime in which we operate, the ratio R_{on}/R_{off} is equivalent to the ratio of the total cross-sections in each case, that is, σ_{on}/σ_{off}. This sequence is repeated several times at several PDL wavenumbers. The analysed data (Methods) are plotted in Fig. 2b. These data are compared with a control analysis at each wavelength, which compares measurements for which the MOT remained on or off for both points, and the computed ratio should thus be consistent with unity (Methods). From this comparison, it is clear that the deviation of the actual data is the result of MOT-induced vibrational relaxation.

To quantify the degree of cooling, we use a simple rate equation model that incorporates both the continual redistribution of the molecules' internal states due to black-body radiation throughout the experiment and the MOT-induced vibrational relaxation when the MOT is present (Methods and Supplementary Information). Because the MOT density and overlap with the ions vary for each of the data points in Fig. 2b, a best-fit line using the rate equation is unsuitable. Rather, using the calculated effective density[26] for each data point, along with the rate equation model, we determine an average vibrational quenching rate constant of $k \approx 1 \times 10^{-9}\,cm^3\,s^{-1}$. Using this rate constant with the typical peak MOT atomic density of $\sim 1 \times 10^9\,cm^{-3}$ and a typical overlap factor of 0.2 (Methods), we calculate the average expected values of R_{on}/R_{off} as predicted from the rate equation model (Fig. 2b, blue curve). Because the data agree well with this curve, we use the rate equations to extract the vibrational ground-state population, which in the case of sympathetic cooling by the Ca MOT is found to be $P_{v=0} \geq 90\%$, set by the competition of sympathetic cooling and black-body radiation heating from the chamber walls. In contrast, if the MOT had provided no cooling, the data would have been consistent with the black line in Fig. 2b, which corresponds to a vibrational ground state population of ~79%.

To our knowledge, rigorous quantum scattering calculations of the vibrational quenching rate have never been performed in any similar system. However, the large value of the rate constant, which is more than 10^4 times that observed in traditional sympathetic cooling schemes, is probably due to the strong, long-range C_4/R^4 interaction potential between Ca and $BaCl^+$ ($C_4 = -\alpha_{Ca}e^2$, where α_{Ca} is the polarizability of Ca). Classically, particles colliding on this potential with energy E and an impact parameter less than the Langevin length, $b_L = \sqrt{C_4/E}$ undergo violent collision trajectories that rapidly spiral

inward towards $R = 0$. Quantum mechanically speaking, the system forms a three-body collision complex with reduced mass μ at the Langevin rate, $k_L = \pi\sqrt{2C_4/\mu}$, which facilitates redistribution of the original molecule's vibrational energy between all three particles. Thus, when the collision complex predissociates back into its parent constituents, this energy is carried away by the sympathetic cooling partner, leaving the molecule in a lower vibrational state. The fact that the observed rate constant is of the same order as the Langevin rate ($k \approx k_L/5$) supports this interpretation[12] and suggests that sympathetic cooling of molecular internal degrees of freedom will be possible with any collision partner that gives rise to long-range interactions conducive to collision complex formation, for example dipole–dipole and monopole–dipole collisions.

Additionally, we have observed no evidence of any chemical reactions between $BaCl^+$ and electronically excited Ca atoms in the MOT, even though such reactions are energetically allowed. This supports the arguments of refs 27, 29, which state that these collisions are suppressed because the long-range atom–ion interaction shifts the atom out of resonance with the atomic cooling laser at large atom–ion separations and thus prevents atoms in their electronically excited state from colliding with the molecular ions. This also provides an important simplification to the originally proposed method[23], because it eliminates the need for an optical dipole trap for the ultracold atoms. Furthermore, it implies that the rate at which sympathetic cooling collisions occur can be increased without loss of molecules. Several straightforward experimental modifications, such as modifying the ion trap geometry such that the ion cloud is fully contained inside the Ca MOT and replenishing the Ca atom source, are expected to increase the effective Ca MOT density and, as a result, the sympathetic cooling collision rate by a factor of ~250. Such improvements would produce a vibrational ground-state population greater than 99% in less than 100 ms, and would potentially render the currently used Ba^+ translational sympathetic cooling unnecessary.

Finally, owing to incomplete spectroscopic information on the $BaCl^+$ molecule, direct measurement of rotational energy quenching is currently not possible. However, because all evidence from sympathetic cooling systems used so far shows that collisional quenching of the rotational energy proceeds at a much higher rate than vibrational quenching, it is likely that molecules have been cooled rotationally as well; experiments are currently underway to prove this. Ultimately, the minimum rovibrational temperature attainable with this method will be set by the ion radial micromotion, which determines the lowest collision energy with the Ca atoms. This collision energy can be estimated from the amplitude of the micromotion, which is given as a function of electric field as $a_{mm} = \sqrt{2}eE(r)/m\omega\Omega$, where ω and Ω are respectively the secular and drive frequencies[30]. The average micromotion kinetic energy ($mv_{mm}^2/2 = m(a_{mm}\Omega)^2/2$, where m is the ion mass and v_{mm} is the component of the ion velocity due to micromotion) over a typical cloud profile in our apparatus for typical trap parameters (that is, a radial pseudo-potential of depth ~10 eV), is ~1 K, whereas the maximum possible micromotion contribution to a collision (for ions residing at the edge of the cloud) is ~10 K. Because the $BaCl^+$ vibrational splitting corresponds to ~500 K, this energy is inconsequential for vibrational cooling. However, the $BaCl^+$ rotational splitting is ~0.5 K, meaning that in the present experiment the lowest few rotational levels could still be populated. Therefore, future experiments aiming to produce samples of molecules purely in the rovibrational ground state should use smaller samples of molecular ions, so that the cloud size and, thus, the micromotion are reduced to the point where collision energies are below the molecular rotational splitting energy. In the present experiment, we estimate that this regime can be reached by working with a sample of order one-tenth the size of the current cloud.

We have demonstrated a broadly applicable, general technique to cool the vibrational motion of polar molecules. We have also developed a general technique, photodissociation thermometry, for probing molecular vibrational states, which we have used to determine the vibrational quenching rate constant and the vibrational ground-state population. This result opens a new route to the production of ultracold molecules and is expected to enable myriad experiments in quantum chemistry[1–3], precision tests of fundamental physics[31], and quantum information and simulation[4,5].

METHODS SUMMARY

The data acquisition system takes an alternating sequence of data points for which the MOT is either on or off during the measurement, and acquires over 100 data points at each PDL wavelength. For each wavelength, the ratio of successive points (R_{on}/R_{off}) is computed to eliminate unidentified time varying systematic errors, and the results are averaged. For the control analysis, the ratios between successive data points of the same type (for example $R_{on,1}/R_{on,2}$, $R_{off,1}/R_{off,2}$ and so on) are instead computed and the results are averaged. See Methods for details.

The production of Ba^+ ions in the experiment is modelled using a simple rate equation model that includes the lowest four vibrational levels of the $BaCl^+$ molecules and accounts for population redistribution among the levels throughout the experimental sequence. This redistribution of the levels is due to collisions with the ultracold Ca atoms as well as spontaneous and stimulated emission and absorption of photons by the molecules owing to the black-body radiation field. Because knowledge of the dipole moment of the electronic ground state of $BaCl^+$ is necessary to determine the spontaneous and stimulated emission and absorption rates, we calculated the dipole moment using a non-relativistic, multiconfigurational, second-order perturbation theory (CASPT2) implemented in the MOLCAS software suite. The result is shown in Fig. 1b. See Methods for details.

Full Methods and any associated references are available in the online version of the paper.

Received 9 October 2012; accepted 23 January 2013.

1. Smith, D. The ion chemistry of interstellar clouds. *Chem. Rev.* **92,** 1473–1485 (1992).
2. Balakrishnan, N. & Dalgarno, A. Chemistry at ultracold temperatures. *Chem. Phys. Lett.* **341,** 652–656 (2001).
3. Krems, R. V. Cold controlled chemistry. *Phys. Chem. Chem. Phys.* **10,** 4079–4092 (2008).
4. André, A, *et al.* A coherent all-electrical interface between polar molecules and mesoscopic superconducting resonators. *Nature Phys.* **2,** 636–642 (2006).
5. Schuster, D., Bishop, L., Chuang, I., DeMille, D. & Schoelkopf, R. Cavity QED in a molecular ion trap. *Phys. Rev. A* **83,** 012311 (2011).
6. Kozlov, M. G. & Labowsky, L. Z. Parity violation effects in diatomics. *J. Phys. At. Mol. Opt. Phys.* **28,** 1933–1961 (1995).
7. Vutha, A. C. *et al.* Search for the electric dipole moment of the electron with thorium monoxide. *J. Phys. At. Mol. Opt. Phys.* **43,** 074007 (2010).
8. DeMille, D. *et al.* Enhanced sensitivity to variation of m_e/m_p in molecular spectra. *Phys. Rev. Lett.* **100,** 043202 (2008).
9. Chin, C., Flambaum, V. V. & Kozlov, M. G. Ultracold molecules: new probes on the variation of fundamental constants. *N. J. Phys.* **11,** 055048 (2009).
10. Hudson, E. *et al.* Production of cold formaldehyde molecules for study and control of chemical reaction dynamics with hydroxyl radicals. *Phys. Rev. A* **73,** 063404 (2006).
11. Krems, R. V., Stwalley, W. C. & Friedrich, B. (eds) *Cold Molecules: Theory, Experiment, Applications* Ch. 13, 18 (CRC, 2009).
12. Ferguson, E. E. Vibrational quenching of small molecular ions in neutral collisions. *J. Phys. Chem.* **90,** 731–738 (1986).
13. Chou, C. W., Hume, D. B., Koelemeij, J. C. J., Wineland, D. J. & Rosenband, T. Frequency comparison of two high-accuracy Al^+ optical clocks. *Phys. Rev. Lett.* **104,** 070802 (2010).
14. McGuirk, J., Foster, G., Fixler, J., Snadden, M. & Kasevich, M. Sensitive absolute-gravity gradiometry using atom interferometry. *Phys. Rev. A* **65,** 033608 (2002).
15. Griffith, W. *et al.* Improved limit on the permanent electric dipole moment of ^{199}Hg. *Phys. Rev. Lett.* **102,** 101601 (2009).
16. Levin, K., Fetter, A. L. & Stamper-Kurn, D. M. (eds) *Ultracold Bosonic and Fermionic Gases* (Elsevier, 2012).
17. Shuman, E. S., Barry, J. F. & Demille, D. Laser cooling of a diatomic molecule. *Nature* **467,** 820–823 (2010).
18. Hummon, M., Yeo, M., Stuhl, B., Xia, Y. & Ye, J. Direct laser cooling of yttrium monoxide. *Bull. Am. Phys. Soc.* **57,** abstr. C2.00002 (2012).
19. Ostendorf, A, *et al.* Sympathetic cooling of complex molecular ions to millikelvin temperatures. *Phys. Rev. Lett.* **97,** 243005 (2006).
20. Staanum, P. F. Højbjerre, K. Skyt, P. S., Hansen, A. K. & Drewsen, M. Rotational laser cooling of vibrationally and translationally cold molecular ions. *Nature Phys.* **6,** 271–274 (2010).
21. Schneider, T., Roth, B., Duncker, H., Ernsting, I. & Schiller, S. All-optical preparation of molecular ions in the rovibrational ground state. *Nature Phys.* **6,** 275–278 (2010).

22. Tong, X., Winney, A. & Willitsch, S. Sympathetic cooling of molecular ions in selected rotational and vibrational states produced by threshold photoionization. *Phys. Rev. Lett.* **105,** 143001 (2010).
23. Hudson, E. Method for producing ultracold molecular ions. *Phys. Rev. A* **79,** 032716 (2009).
24. Chen, K. *et al.* Molecular-ion trap-depletion spectroscopy of $BaCl^+$. *Phys. Rev. A* **83,** 030501 (2011).
25. Schowalter, S. J., Chen, K., Rellergert, W. G., Sullivan, S. T. & Hudson, E. R. An integrated ion trap and time-of-flight mass spectrometer for chemical and photo-reaction dynamics studies. *Rev. Sci. Instrum.* **83,** 043103 (2012).
26. Rellergert, W. *et al.* Measurement of a large chemical reaction rate between ultracold closed-shell ^{40}Ca atoms and open-shell $^{174}Yb^+$ ions held in a hybrid atom-ion trap. *Phys. Rev. Lett.* **107,** 243201 (2011).
27. Sullivan, S. T., Rellergert, W. G., Kotochigova, S. & Hudson, E. R. Role of electronic state excitation in ground-state-forbidden inelastic collisions between ultracold atoms and ions. *Phys. Rev. Lett.* **109,** 223002 (2012).
28. DeVoe, R. Power-law distributions for a trapped ion interacting with a classical buffer gas. *Phys. Rev. Lett.* **102,** 063001 (2009).
29. Band, Y. & Julienne, P. Optical-Bloch-equation method for cold-atom collisions: Cs loss from optical traps. *Phys. Rev. A* **46,** 330–343 (1992).
30. Major, F. G. & Dehmelt, H. G. Exchange-collision technique for the rf spectroscopy of stored ions. *Phys. Rev.* **170,** 91–107 (1968).
31. Leanhardt, A. *et al.* High-resolution spectroscopy on trapped molecular ions in rotating electric fields: a new approach for measuring the electron electric dipole moment. *J. Mol. Spectrosc.* **270,** 1–25 (2011).

Supplementary Information is available in the online version of the paper.

Acknowledgements This work was supported by ARO grant no. W911NF-10-1-0505, US NSF grant nos PHY-1005453 and PHY-1205311, and AFOSR grant no. FA 9550-11-1-0243.

Author Contributions E.R.H., W.G.R. and S.T.S. conceived of the thermometry technique and measurement protocol. W.G.R. and S.T.S. built the MOTion trap apparatus, wrote the data acquisition software, and acquired and analysed all data in Fig. 2. S.J.S. built the time-of-flight apparatus, acquired and analysed the data in Fig. 1, and helped K.C. write the data acquisition software for these data. S.K. calculated the potential energy curves and dipole moment for the $BaCl^+$ molecules as well as the relevant absorption, spontaneous and stimulated emission rates due to black-body radiation. S.J.S. prepared all of the figures. W.G.R. wrote the manuscript with input from all authors.

Author Information Reprints and permissions information is available at www.nature.com/reprints. The authors declare no competing financial interests. Readers are welcome to comment on the online version of the paper. Correspondence and requests for materials should be addressed to W.G.R. (wgr6@ucla.edu).

METHODS

To eliminate several sources of systematic error when comparing our data with the rate equation model, for example the variable number of $BaCl^+$ ions produced in the loading process and possible inaccuracies in the absolute cross-section value, the PDL intensity or both, we use the fluorescence as a measure of the number of Ba^+ ions created in each instance of photodissociation and calculate the ratio of the final amount to the initial amount, $R_{on} = N_2/N_1$ (Fig. 2a). We then repeat this measurement sequence without turning on the Ca MOT, and record the same ratio, which we denote R_{off}. It is straightforward to show that in the linear regime in which we operate the ratio R_{on}/R_{off} is equivalent to the ratio of the total cross-sections in each case, that is, σ_{on}/σ_{off}. We repeat this entire sequence >50 times and thus obtain a series of data points $R_{on,1}$, $R_{off,1}$, $R_{on,2}$, $R_{off,2}$, …. To eliminate monotonic, time-varying systematic errors, we compute and average the ratios $R_{on,1}/R_{off,1}$, $R_{on,2}/R_{off,2}$, … as well as the ratios $R_{on,2}/R_{off,1}$, $R_{on,3}/R_{off,2}$, …. We then average the two results and repeat the experiment at various photodissociation wavelengths. These data are plotted as blue circles in Fig. 2b. Also plotted (black circles) are the results of a control analysis in which we instead perform the same calculation for the ratios $R_{on,1}/R_{on,2}$, $R_{on,3}/R_{on,4}$, … as well as $R_{off,1}/R_{off,2}$, $R_{off,3}/R_{off,4}$, … and average the results. Because these controls are comparisons of the same data type, they should yield results consistent with unity, and their variability about this value can be used as an indication of the variability in the actual data. Their close agreement with unity shows that the deviation from unity of the true data is due to MOT-induced vibrational relaxation and is not a statistical coincidence.

The number of Ba^+ ions created in each instance of photodissociation can be obtained using the following rate equations:

$$\frac{dN_i}{dt} = \rho\Phi(k_{i+1,i}N_{i+1} - k_{i,i-1}N_i) - \frac{\sigma_i(\lambda)I}{h\nu}N_i + \sum_{j>i}A_{ji}N_j - \sum_{j<i}A_{ij}N_i + \sum_{j\neq i}B_{ij}\rho(\omega)(N_j - N_i) \quad (2)$$

$$\frac{dN_{Ba}}{dt} = \sum_i \frac{\sigma_i(\lambda)I}{h\nu}N_i$$

Here N_i denotes the number of $BaCl^+$ molecules in the ith vibrational level (we have averaged over the rotational states) and N_{Ba} is the number of Ba^+ ions.

The first term in the expression for dN_i/dt (equation (2)) is due to the MOT-induced quenching: $k_{i+1,i}$ is the vibrational quenching rate constant for transition from the $(i+1)$th level to the ith level, ρ is the peak density of the MOT and Φ is a factor that quantifies the degree of overlap of the atom and ion clouds. We define $\Phi = \int \hat{\rho}_{Ca}(r)\bar{\rho}_I(r)\,dr$, where $\hat{\rho}_{Ca}$ is the unit-peak normalized Ca atom density and $\bar{\rho}_I$ is the unit-integral normalized $BaCl^+$ density. Thus, $0 < \Phi < 1$. In the liquid phase in which we operate, Φ quantifies the effective MOT density experienced by each ion as they move in the trap.

The second term in the expression for dN_i/dt results from photodissociation (σ_i is the wavelength-dependent cross-section for the ith level, I is the PDL intensity and ν is the laser frequency). The last three terms are due to spontaneous emission and BBR-induced stimulated emission and absorption written in terms of the spectral energy density, $\rho(\omega)$, and the Einstein A and B coefficients[32].

Calculating these coefficients requires knowledge of the dipole moment of the electronic ground state of $BaCl^+$, $A_{ij} = (2/3)(\omega_{ij}^3\mu_{ij}^2/\varepsilon_0 hc^3)$, where $\mu_{ij} = \langle j|d(R)|i\rangle$, $|n\rangle$ represents the rovibrational wavefunction of the nth rovibrational level of the ground electronic state, ω_{ij} is the angular frequency of the transition, ε_0 is the vacuum permittivity and c is the speed of light. We calculated this dipole moment function, which was previously unknown, using a non-relativistic, multiconfigurational, second-order perturbation theory (CASPT2) implemented in the MOLCAS software suite. The result is shown in Fig. 1b. With this in hand, the necessary rates are calculated according to ref. 32, and are ~1 Hz. Finally, we incorporate the lowest four vibrational levels into the model and ignore terms where $|i-j| > 1$. This model, along with the calculated effective density of the MOT[26] for each data point, allows a determination of the vibrational quenching rate constant, k, as well as the ground-state vibrational population, $P_{v=0}$.

32. Lefebvre-Brion, H. & Field, R. W. *The Spectra and Dynamics of Diatomic Molecules* Ch. 5 (Academic, 2004).